

# An achiral, anticlinic-promoting, smectic liquid crystal architecture

Jirakorn Thisayukta and Edward T. Samulski\*

Department of Chemistry, University of North Carolina, Chapel Hill, NC, 27599-3290, USA. E-mail: et@unc.edu; Fax: 919-962-2388; Tel: 919-962-1561

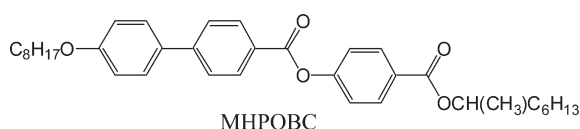
Received 20th January 2004, Accepted 18th March 2004  
First published as an Advance Article on the web 26th April 2004

We describe a simple, achiral, terminal chain that appears to readily convert the synclinc SmC phase to the anticlinic SmC<sub>A</sub> phase. If the  $\alpha$ -carbon of a terminal chain is di-substituted, *i.e.*, if either 1,1-dimethylpentylloxycarbonyl or 1,1-dimethylhexylloxycarbonyl is used instead of the usual chiral chain, 1-methylheptyloxycarbonyl, the terminal chain in the well known, antiferroelectric mesogen MHPOBC, an anticlinic SmC<sub>A</sub> phase is observed exclusively below the SmA phase. Moreover, the dimethyl-substituted terminal chain can induce the SmC<sub>A</sub> phase in very ordinary mesogens: *n*-hexyl decyloxybiphenyl carboxylate (HDBC) changes its conventional synclinc SmC phase into the anticlinic SmC<sub>A</sub> phase when mixed with a molecule having the same HDBC core but containing the dimethyl-substituted terminal chain. The simple structure of this achiral terminal chain suggests that a generic mechanism is responsible for tilt sense propagation in smectics: we posit that subtle intra-layer packing arrangements within the aliphatic stratum give rise to a topographic pattern on the layer interface, and that this pattern communicates tilt sense preferences, anticlinic or synclinc, from layer to layer.

## Introduction

The first proposal of a tilted smectic C phase having its tilt director, **c**, alternate from +**c** to -**c** on translating from layer to layer—an anticlinic stacking motif—was for a mainchain polymer liquid crystal.<sup>1</sup> Therein the polymer secondary structure—the parity of the spacer chain as idealized in Fig. 1a—dictates an alternation in the orientation of successive mesogenic cores along the polymer backbone. Even spacer chains promote either the normal smectic A phase, with mesogens aligned parallel to the layer normal **N**, or a synclinc phase, with mesogens in adjacent layers tilted in the same direction relative to **N** (Fig. 1b). By contrast, odd parity spacers promote an anticlinic stacking motif.<sup>1</sup>

Since the discovery of the antiferroelectric, chiral, smectic C phase (SmC<sub>A</sub><sup>\*</sup>) in the low molar mass liquid crystal MHPOBC,<sup>2</sup> 4-(1-methylheptyloxycarbonyl)-phenyl 4'-octyloxybiphenyl-4-carboxylate, there has been a concerted effort to understand the origins of the anticlinic stacking motif. Since its discovery in MHPOBC, the SmC<sub>A</sub><sup>\*</sup> phase has been observed in numerous other smectics.<sup>3</sup> Threshold-less (“V-shaped”) switching and its implications for displays<sup>4</sup> is one technologically important aspect of the SmC<sub>A</sub><sup>\*</sup> phase. Such technical motivation as well as interest in stratified phases generally, have prompted a variety of proposals for why the anticlinic stacking motif is stabilized relative to the synclinc motif found in conventional SmC and SmC<sup>\*</sup> phases.



In early modeling of the interactions that might promote the SmC<sub>A</sub><sup>\*</sup> phase in MHPOBC, Takanishi *et al.*<sup>5</sup> proposed that pairing of “transverse electrostatic dipoles” (on identical enantiomers) across the smectic layer interface stabilized the anticlinic arrangement in these chiral mesogens. But in order to rationalize the observation of the anticlinic arrangement in the smectic-C phase of racemic mixtures (denoted SmC<sub>A</sub>), this model necessitates the spontaneous segregation of enantiomers into domains of uniform chirality (spontaneous optical resolution) in order to enable the explicit dipolar pairing between

enantiomers across the smectic interface boundary. The idea that the anticlinic stacking originates from electrostatic interactions across the layer interface in the SmC<sub>A</sub><sup>\*</sup> phase was reinforced by the “bent terminal chain conformation” observed in the crystal structure of MHPOBC.<sup>6</sup> This local conformation results in an obliquely oriented terminal chain which in turn, gives shorter distances between paired dipoles across the layer. However, the persistence of the bent terminal chain conformation in the mesophase of this class of molecules has been called into question:<sup>7</sup> it is *not* the lowest energy conformation of the chain and its existence in the solid state appears to be due to extra-molecular crystal packing considerations. In fact, Toriumi *et al.* show that the obliquely oriented terminal chain appears to reconfigure itself and extend in a conventional manner along the mesogen’s “long axis” in molecular dynamics simulations of stratified phases of MHPOBC. The requirement of pair-wise dipolar interactions between identical enantiomers (and the necessity of spontaneous optical resolution in racemates) is avoided in molecular-statistical theories wherein interlayer *dipole orientational correlations* between bent, polar, terminal chains are hypothesized<sup>8</sup> to be the stabilizing source of the anticlinic packing motif. However, it is not obvious why for the MHPOBC homologues, the interlayer dipole orientational correlations should depend in an erratic manner on the parity or lengths of the both the “inactive” achiral chain, *m*, and “active” chiral chain, *n* (see Fig. 2). Focusing for example, on a

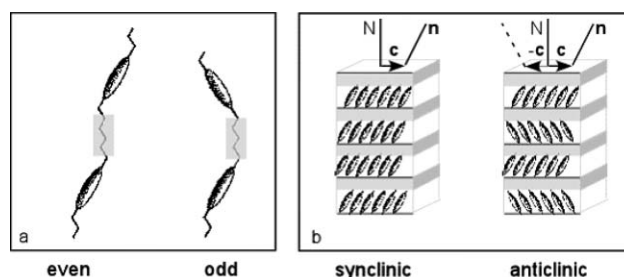


**Fig. 1** Polymer secondary structural implications in tilted smectic stacking motifs. a: Mainchain polymers with even and odd parity spacer chains; b: Stacking motifs: synclinc for even parity spacers and anticlinic for odd parity spacers. **N** is the normal to the smectic layers, **n** the (local) primary director, and **c** is the tilt director.

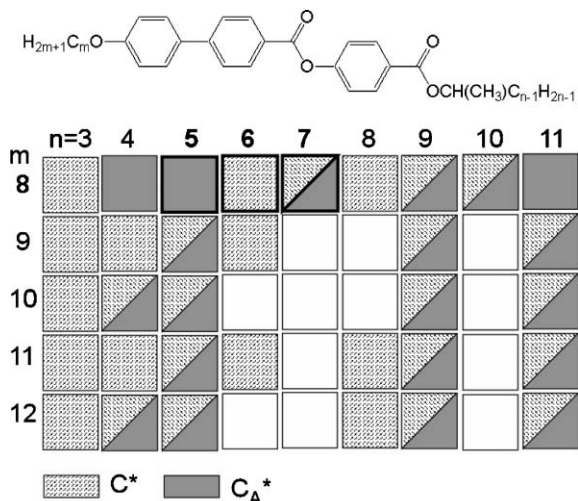


**Fig. 2** The frequency of occurrence of the anticlinic packing motif ( $\text{SmC}_A^*$  phase) with normal alkyl tail length ( $m$ ) and "active" chiral tail ( $n$ ) among homologues of the MHPOBC mesogens (after Fukuda *et al.*<sup>9</sup>). MHPOBC ( $m = 8, n = 7$ ) exhibits a  $\text{SmC}^*$  phase followed by a lower temperature  $\text{SmC}_A^*$  phase; this latter phase sequence is the commonly observed one. In our study we replicate the reported findings for  $m = 8, n = 5, 6$  and  $7$ .

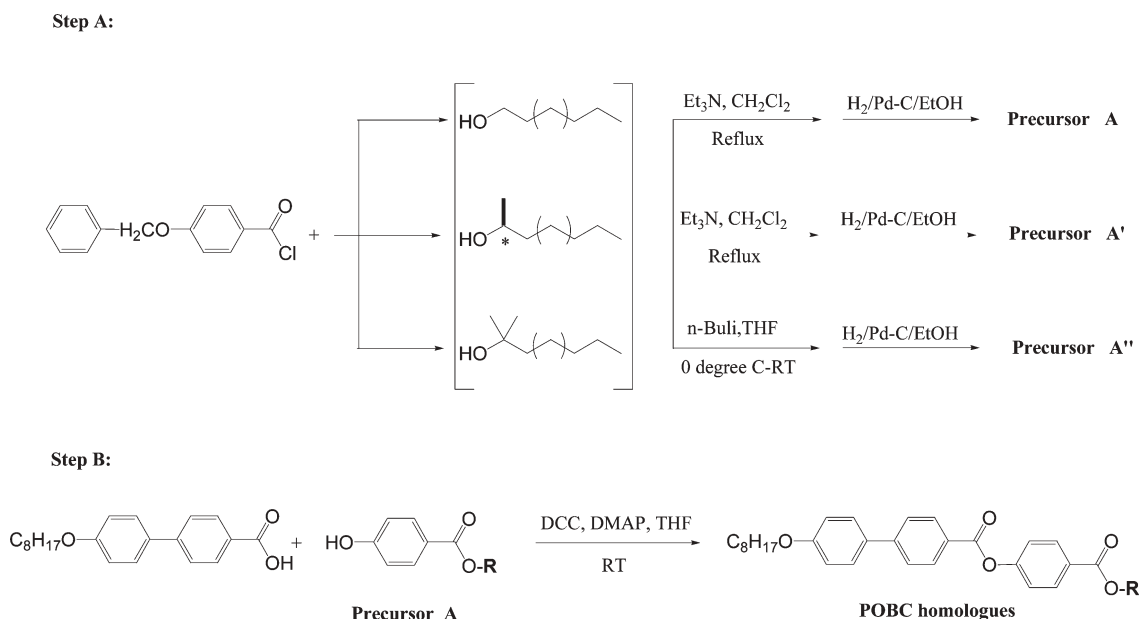
fixed achiral chain length  $m = 8$ , some homologues of MHPOBC exhibit only the conventional  $\text{Sm-C}^*$  phase ( $m = 8, n = 3, 6, 8$ ), others only the  $\text{Sm-CA}^*$  phase ( $m = 8, n = 4, 5, 11$ ), and some exhibit both  $\text{Sm-C}^*$  and  $\text{Sm-CA}^*$  phases ( $m = 8, n = 5, 7, 10$ )<sup>9</sup> Additionally, there are non-electrostatic proposals for the origin of the anticlinic stacking motif: achiral "swallowtail" smectogens also exhibit the anticlinic motif and there the origins of alternating tilt were suggested to derive from steric considerations—interlayer interdigitation of single and branched terminal chains.<sup>10</sup> More recently Glaser and Clark<sup>11</sup> suggest that quenching of out of layer fluctuations and interlayer interdigitation in artificially tilted strata of spherocylinders underlies the propensity for anticlinic motifs. However, they show that such fluctuations are hindered for large tilt angles and appear to stabilize anticlinicity only for small tilts. This prediction leads one to infer from the model that the phase sequence anticipated with increasing tilt (decreasing

temperature) should be  $\text{Sm-C}_A$  followed by  $\text{Sm-C}$ , in conflict with all known experimental phase sequences.

It is in this context of unresolved speculation about the origin of the anticlinic stacking motif in tilted smectics that we report a new, achiral terminal tail architecture—dimethyl substitution on the  $\alpha$ -carbon of the "active" tail—that induces the  $\text{Sm-C}_A$  phase in molecules having either the MHPOBC mesogenic core or the much simpler biphenyl carboxylate core. We initially focus on MHPOBC analogues as these materials have been thoroughly studied, but more importantly, replicating findings on known  $\text{Sm-C}_A^*$  materials gives us a secure platform for illustrating the role of the dimethyl substituted tail. To that end we re-synthesized several MHPOBC homologues ( $m = 8; n = 5, 6, 7$ ) in order to confirm the phase types of the MHPOBC mesogens and provide a context for the new mesogens reported here. As the  $m = 8$  homologue with  $n = 5$  exhibits only the anticlinic  $\text{Sm-C}_A^*$  phase, that with  $n = 6$  the  $\text{Sm-C}^*$  phase only, and that with  $n = 7$  (MHPOBC) both, a high temperature  $\text{Sm-C}^*$  followed by the  $\text{Sm-C}_A^*$ , re-examining these homologues enabled us to insure that we could differentiate between the  $\text{Sm-C}_A$  and  $\text{Sm-C}$  phases. This in turn enabled us to unambiguously demonstrate the role of the dimethyl substituted tail. Finally, we show that anticlinic stacking can also be induced by the dimethyl substituted tail in molecules having a conventional smectogenic core (a simple biphenyl core). We thereby explicitly illustrate that the anticlinicity derives from the tail architecture, a test rarely performed when evaluating the influence of other tail architectures on anticlinicity.

## Experimental

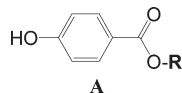
Transition temperatures were determined by using a Seiko DSC 120 differential scanning calorimeter. The second heating ( $10\text{ }^\circ\text{C min}^{-1}$ ) as well as the cooling scans ( $10\text{ }^\circ\text{C min}^{-1}$ ) were recorded. The mesophases were identified with a Nikon Microphot-FX polarizing microscope equipped with a Linkam hotstage. X-Ray measurement was carried out using an Enraf Nonius diffractometer (FR590,  $\text{CuK}\alpha$ , 30 mA, 40 KV). The samples were mounted on a hot stage connected with a temperature control (Mettler Toledo FP90HT.) The general synthetic strategy for preparing mesogens with the MHPOBC core is shown in Scheme 1. In the first step, the esterified phenol (precursor A) was prepared with R determined by the alcohol used in this step. The chiral alcohols (*R*)-(-)-2-hexanol, (*R*)-(-)-2-heptanol, and



**Scheme 1** General synthetic route to POBC mesogens.

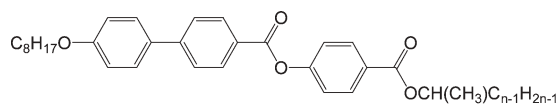
**Scheme 1** General synthetic route to POBC mesogens.

(*R*)-(-)-2-octanol, were used to prepare precursor A for the MnPOBC series ( $n = 5,6,7$ ). The two dimethyl-substituted alcohols 2-methyl-2-hexanol (Aldrich) and 2-methyl-2-heptanol (Lancaster) needed to prepare precursor A for DM5POBC and DM6POBC were used without further purification. And the corresponding normal alcohols were used in the preparation of the *n*POBC mesogens. Precursor A was reacted with the octyloxy-terminated biphenyl carboxylic acid in step B to complete the synthesis of homologues containing the POBC core.

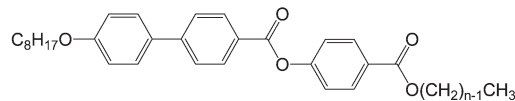


## Results and discussion

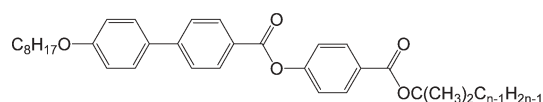
We try to facilitate the discussion by formulating a consistent set of mnemonics to specify homologues while at the same time recognizing the wide-spread usage of the abbreviation “MHPOBC.” In order to do this we adopt acronyms that specify the number of carbons,  $n$ , in the primary “arm” of the “active” (ester-linked) terminal chain of POBC-based mesogens. In our proposed notation homologues of the (chiral) methyl-substituted, active terminal chains are designated *Mn*POBC. The methyl carbon is not counted in the specification of  $n$ , and hence M7POBC becomes the new label for MHPOBC. We use *n*POBC to designate the achiral, normal (unsubstituted) alkyl ester homologues. Finally, *DMn*POBC specifies a homologue having a dimethyl-substituted  $\alpha$ -carbon in its ester terminal chain.



**MnPOBC**



***n*POBC**



**DMnPOBC**

In order to confirm the identity of the  $\text{SmC}_A^*$  phase in the new mesogens synthesized in this investigation, we have repeated the synthesis of some mesogens already reported in the *Mn*PBOC family with  $m = 8$  (bold squares in Fig. 2). In Fig. 3 and Table 1 (rows 1–3), we show the transition maps for *Mn*PBOC ( $n = 5,6,7$ ). Fukuda *et al.* reported earlier an odd–even occurrence of the  $\text{SmC}_A^*$  phase for a fixed length of the ether-linked, achiral, chain—the octyloxy tail ( $m = 8$ )—is most prominent in moderate lengths of the chiral ester-linked chain ( $n = 4–8$ ).<sup>9</sup> We

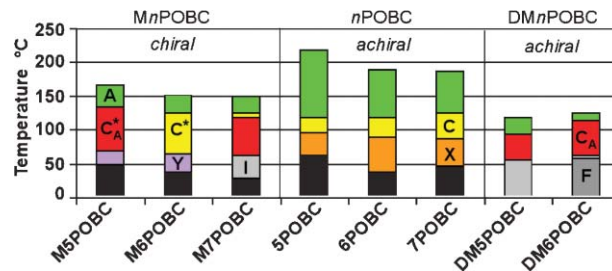
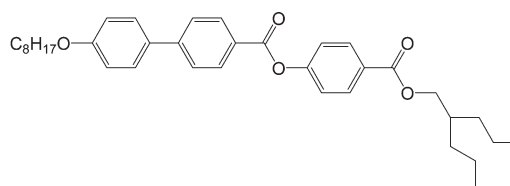


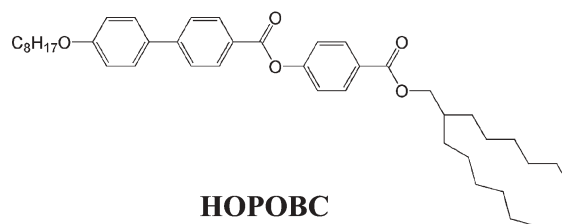
**Fig. 3** Transition maps for three classes of POBC homologues. 1) *Mn*POBC,  $n = 5,6,7$  (M7POBC is usually referred to as MHPOBC); 2) the unsubstituted, active chain for  $n = 5,6,7$  in *n*POBC mesogens; 3) the dimethyl-substituted active chain mesogens *DMn*POBC. The abbreviations Cr, A, C, C\* correspond to crystal, smectic-A, synclinc stacking motifs of the achiral and chiral smectic-C phases, and  $\text{C}_A$  and  $\text{C}_A^*$  to the anticlinic achiral and chiral smectic-C phases, respectively; other less common and/or incompletely characterized low temperature smectics are symbolized with X, Y.

corroborated this alternation in the appearance of the  $\text{SmC}_A^*$  for *Mn*PBOC ( $n = 5,6,7$ ) mesogens. The related achiral homologues *n*PBOC ( $n = 5,6,7$ ) synthesized from the normal alcohols exhibit only the synclinc SmC phase independent of terminal chain parity (Table 1 rows 4–6, and Fig. 3 middle section). The absence of a chiral center in the *n*PBOC series is expected to perturb both the magnitude of the electrostatic dipole moment on the ester-linked terminal chain and the chain’s (average) conformation. Hence it is not possible to infer the origins of the anticlinic stacking motif—electrostatic or steric—from the different behavior of the *n*PBOC series relative to the *Mn*PBOC series as more than one attribute of the mesogens is being perturbed by this change in the primary structure of the active tail.



**PPOBC**

Cr  $\leftarrow$  70 °C  $\rightarrow$  SmC  $\leftarrow$  118 °C  $\rightarrow$  SmA  $\leftarrow$  145 °C  $\rightarrow$  I



**HOPOBC**

Cr  $\leftarrow$  25 °C  $\rightarrow$  SmC  $\leftarrow$  80 °C  $\rightarrow$  SmA  $\leftarrow$  118 °C  $\rightarrow$  I

**Table 1** Phases and transitions (°C) for POBC derivatives

Mesogen\Phase	Cr	$T_{mp}$	F	$T_m$	I	$T_m$	Y	$T_m$	X	$T_m$	$\text{C}_A$	$T_m$	C	$T_m$	A	$T_{cl}$
<b>M5POBC</b>	●	50	—	—	—	—	●	70	—	—	●	134	—	—	●	167
<b>M6POBC</b>	●	37	—	—	—	—	●	65	—	—	—	—	●	126	●	152
<b>M7POBC</b>	●	30	—	—	●	63	—	—	—	—	●	118	●	125	●	150
<b>5POBC</b>	●	63	—	—	—	—	—	●	97	—	—	—	●	119	●	220
<b>6POBC</b>	●	38	—	—	—	—	—	●	90	—	—	—	●	119	●	190
<b>7POBC</b>	●	46	—	—	—	—	—	●	88	—	—	—	●	125	●	187
<b>DM5POBC</b>	—	<20	—	—	●	55	—	—	—	—	●	93	—	—	●	119
<b>DM6POBC</b>	—	<20	●	59	●	63	—	—	—	—	●	114	—	—	●	125

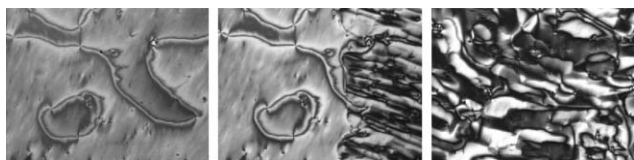


**Fig. 4** The evolution of the SmC texture (left) on lowering the temperature in a mixture of 6POBC and DM6POBC. The anticlinic SmC<sub>A</sub> phase grows into the SmC phase (center) and eventually dominates the field of view (right) as the temperature is lowered.

The new finding reported here is that the anticlinic SmC<sub>A</sub> phase is readily obtained with the 1,1-dimethyl-substituted ester-linked chains, DM $n$ POBC ( $n = 5, 6$ ). These seemingly innocuous achiral relatives of MHPOBC are easily derived from two commercially available starting alcohols (2-methyl-2-hexanol and 2-methyl-2-heptanol). Both of the new materials exhibit an anticlinic SmC<sub>A</sub> phase. In Fig. 3 (last section) and Table 1 (rows 7 and 8) the transition maps for DM5POBC and DM6POBC show multiple smectic phases with an anticlinic SmC<sub>A</sub> phase between the SmA and the SmI phases. We have observed the onset of the SmC<sub>A</sub> phase in the DM $n$ POBC mesogens on cooling from the SmA phase. Screw-wedge dispirations—a  $\pi$ -wedge disclination ( $m = 1/2$ ) accompanied by a screw dislocation<sup>12,13</sup>—appear in homeotropically aligned samples of both DM5POBC and DM6POBC. Confirmation that these new mesogens exhibit an anticlinic SmC<sub>A</sub> phase is also available from texture studies in mixing experiments with mesogens known to show only SmC phases (e.g.,  $n$ POBC mesogens). Fig. 4 shows the evolution of the SmC texture in a mixture of 6POBC with DM6POBC. On lowering the temperature the SmC phase is unequivocally transformed to the SmC<sub>A</sub> phase. Relative to the MnPOBC mesogens the dimethyl substitution in the terminal chains of DM $n$ POBC markedly lowers the clearing temperature and melting point. Also, the SmA phase appears to be destabilized relative to the SmC<sub>A</sub> phase with increasing length of the dimethyl ester terminal chain (from  $n = 5$  to  $n = 6$ ). Finally for these two homologues the formation of the anticlinic stacking motif is independent of chain parity, in contrast with MnPOBC for  $n = 5$  and 6.

In an attempt to acknowledge work suggesting that swallow-tail terminal chains promote anticlinic packing in other mesogenic cores<sup>10</sup> and related observations with the POBC core,<sup>14</sup> we have prepared two swallow-tail derivatives, PPOBC and HOPOBC. These swallow-tail derivatives differ from earlier reported POBC-based swallow-tails in that the branch point occurs at the  $\beta$ -carbon rather than the  $\alpha$ -carbon. In agreement with observations by Ouchi *et al.*<sup>14</sup> neither the 2-propylpentylloxycarbonyl derivative PPOBC nor the 2-hexyloctylloxycarbonyl derivative HOPOBC exhibits a SmC<sub>A</sub> phase whereas the 1-propylbutylloxycarbonyl terminal tail—the  $\alpha$ -carbon-based swallow tail—on the POBC core was reported to form the anticlinic phase.<sup>13</sup>

In Fig. 5 we contrast the temperature dependence of smectic layer spacing,  $d$ , derived from low-resolution X-ray diffraction for three, 6-carbon, active chain mesogens, 6POBC, M6POBP, and DM6POBC. The horizontal dashed line in each panel corresponds to the length  $L_o$  of the extended all-*trans* conformation of the mesogens. For all three mesogens (each with the same length  $n = 6$  active tail), the idealized length is the same ( $L_o \approx 36.5$  Å); the width of the gray band in the figures corresponds to 2 Å and is intended to emphasize conformational disorder, interdigitation and/or local bend of the terminal tails that presumably accounts for the contraction of  $d$  relative to  $L_o$  in the SmA phase. To within the experimental uncertainty ( $\pm 0.5$  Å), this contraction is of comparable magnitude for all three mesogens although there is some indication that the contraction of  $L_o$  (interdigitation) might be more pronounced in the SmA phase of the straight-chain mesogen 6POBC. One also infers from the X-ray data that the

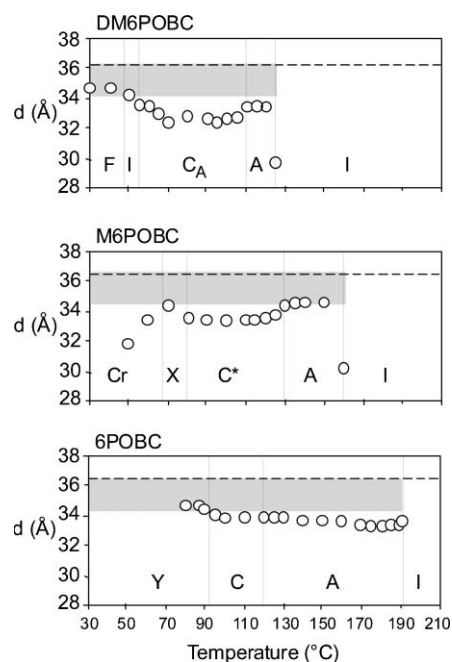
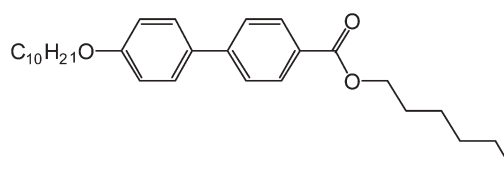


**Fig. 5** Smectic layer spacing  $d$  as a function of temperature for three related mesogens with  $n = 6$  carbons in the active, ester-linked terminal chain, 6POBC, M6POBC, and DM6POBC. The smectic phase types are indicated; Cr is the crystal and  $I$  the isotropic melt.

6POBC mesogen shows very little “tilt” on going from the SmA to SmC phase. However, a higher resolution X-ray study coupled with direct measurements of the optical tilt is essential to ascertain if 6PBOC is a candidate for a de Vries type SmA.<sup>15</sup> The layer spacing change at the SmA-to-tilted smectic for M6POBC (to a SmC\* phase) and for DM6POBC (to a SmC<sub>A</sub> phase) is indicative of a discontinuous change in the tilt at the phase boundary.<sup>16</sup> The contraction of  $L_o$  due to tilt and other mechanisms in the SmC<sub>A</sub> phase of DM6POBC is more pronounced than that in the SmC\* phase of M6POBC (Fig. 5). The magnitude of  $d$  in the crystalline phase of M6POBC is suggestive of interdigitation and a severely bent (oblique) ester-linked chiral tail. This was corroborated by a recent crystal structure determination of M6POBC.<sup>17</sup> But there is no clear X-ray structural signature of the anticlinic stacking observed in the SmC<sub>A</sub> phase of DM6POBC. (We have not looked in detail at the diffraction intensity distribution in such low-resolution patterns to see if relative to the SmC phase, there is a more defined layer structure in our SmC<sub>A</sub> phases.<sup>18</sup>)

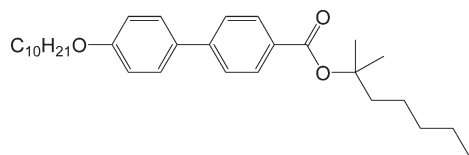
Our observations with the DM $n$ POBC mesogens prompt several questions relating to the potential of this substituted achiral tail for stabilizing the anticlinic stacking motif: is the observation that 1,1-dimethyl terminal tails induce an anticlinic phases in both DM5POBC and DM6POBC just an accident? Is the POBC mesogenic core essential for promoting the anticlinic stacking motif? Or, is anticlinicity (SmC<sub>A</sub> phase formation) promoted by some as yet undefined inter-layer interactions inherent to 1,1-dimethyl tails, irrespective of the chemical constitution of the mesogenic core? In order to begin to answer these questions we examined the role of 1,1-dimethyl tails in a very simple smectogen architecture, *n*-hexyl-4'-decyloxybiphenyl-4-carboxylate (HDBC).



**HDBC**

Cr  $\leftarrow$  60 °C  $\rightarrow$  SmC  $\leftarrow$  63.5 °C  $\rightarrow$  SmA  $\leftarrow$  85 °C  $\rightarrow$  I

This classical calamitic mesogen exhibits conventional smectic phases: a SmA phase and a synclinc SmC phase (see HDHC transition map).<sup>19</sup> When the ester-linked hexyl tail is replaced by a 1,1-dimethyl hexyl tail (DMHDBC), there is a precipitous lowering of the resulting molecule's melting point (to 12 °C) and the liquid crystalline phases are lost. DMHDBC is *not* a thermotropic liquid crystal. Hence, for this simple biphenyl mesogenic core, a direct comparison of the influence of the 1,1-dimethyl-substituted terminal chain on the tilted smectic stacking motif is not possible.



DMHDBC

Cr ← 12 °C → I

However, we are able to observe the stacking motif in the virtual smectic C phase of DMHDBC by examining mixtures of the DMHDBC molecule with the HDHC mesogen. Fig. 6 shows the resulting phase diagram for several molar ratios, HDHC/DMHDBC. The melting and clearing temperatures are decreased with increasing DMHDBC in the mixtures, and the SmA and SmC phase stabilities of HDHC decrease. At 20 mol% DMHDBC a separate anticlinic SmC<sub>A</sub> phase appears and displaces the increasingly unstable synclinc SmC phase as the DMHDBC content increases; the SmC<sub>A</sub> phase persists for about a 25° range in the 50 mol% sample. At higher DMHDBC contents, immiscible SmA and SmC<sub>A</sub> mesophases persist until only the SmA phase is stable at about 70 mol% DMHDBC.

These findings with mixtures of the dimethyl-substituted tail material (DMHDBC) and a conventional mesogen (*e.g.*, HDHC) suggest that an antiferroelectric SmC<sub>A</sub>\* phase might be readily produced by adding a chiral dopant to an appropriate mixture based on a readily available synclinc smectic-C-forming mesogen. There could be related implications for making ferroelectric banana phases by exploiting the anticlinic motif of the dimethyl-substituted tail. A typical banana mesogen such as the pentyloxy derivative or resorcinol,

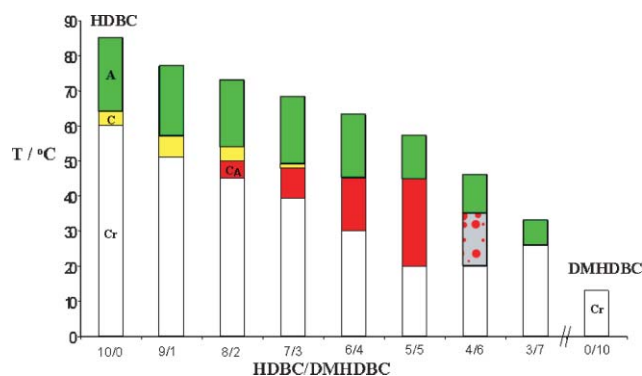
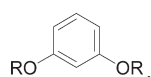
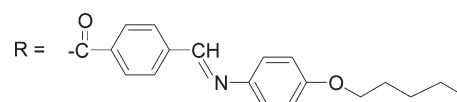


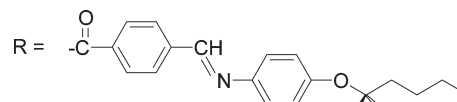
**Fig. 6** Transition maps for HDHC (left), DMHDBC (right), and various molar ratios of HDHC/DMHDBC mixtures; the smectic A, C and C<sub>A</sub> phases are indicated. HDHC exhibits a smectic A phase and a conventional synclinc smectic C phase. A low temperature C<sub>A</sub> phase appears for ratios <8/2, and this C<sub>A</sub> phase eventually disappears at ratios <4/6; only a phase-separated mixture is observed for the 4/6 ratio. DMHDBC does not exhibit a mesophase.

where



Cr ← 176 °C → B<sub>1</sub> ← 181 °C → I

exhibits a B<sub>1</sub> phase.<sup>20</sup> We have preliminary data<sup>21</sup> on the dimethyl-substituted banana where R is:



Cr ← 85 °C → I

Unfortunately, as observed for the calamitic mesogen HDHC, the resulting low-melting banana-shaped molecule does not exhibit a mesophase and its melt supercools to ~20 °C and simply crystallizes. However, such a dramatic lowering of the transition temperature is anticipated from the behaviour of HDHC and DMHDBC. It remains to be seen if mixtures of this dimethyl-substituted bent molecule can induce phase changes in banana mesogens.

## Conclusions

We have shown that the 1,1-dimethyl-substituted, ester-linked terminal chain promotes SmC<sub>A</sub> phase formation for the well known POBC mesogenic core. But this dimethyl-substituted chain also induces a SmC<sub>A</sub> phase in molecules comprised of the simple biphenyl core. The exact molecular mechanism whereby a synclinc rather than an anticlinic stacking motif is generated is still a matter of conjecture. However, when all of the data is viewed as a whole—the somewhat erratic odd–even dependence on *n* (and *m*) of the SmC<sub>A</sub>\* phase in the MnPOBC series (Fig. 2), SmC<sub>A</sub> phase formation in α-carbon-substituted swallow-tail POBC derivatives<sup>14</sup> (but not in β-carbon-substituted ones, *e.g.*, PPOBC and HOPOBC), and the results on dimethyl-substituted tails reported here—it is difficult to make a compelling case that interlayer electrostatic interactions are the origin of the anticlinic stacking motif. In fact it appears that a more generic explanation of the stacking motif is needed.

Random out-of-plane mesogen translation (smectic interface roughness) of the type suggested by Glaser and Clark<sup>11</sup> is an attractive mechanism, but apart from its erroneous prediction of phase sequences, the roughness stemming from random translations of the mesogens within the smectic strata would require more structural details (*e.g.*, minimally bent particles<sup>22</sup>) to begin to address the quasi odd–even appearance of the SmC<sub>A</sub>\* in the POBC homologues. The data in Fig. 2 in conjunction with other reported observations on SmC<sub>A</sub> phase formation demands a more tail-specific mechanism. To that end we speculate that tilt sense from layer-to-layer is communicated *via* topographic patterns formed on the smectic layer interface by “solvation structures”—2-D nearest neighbor tail coordination patterns in the aliphatic strata. The coordination patterns are suggested to derive from preferred packing arrangements of the mesogen's inequivalent tails in the aliphatic strata of the smectic layer. We borrow this speculative proposal from the literature of liquid–liquid immiscibility in membranes—pattern formation of complexes of phospholipids and cholesterol—and its putative role in transbilayer correlations in cell membranes.<sup>23</sup>

In biological membranes, in-plane solvation structures—2-D arrangements of mixed species within one membrane monolayer (leaflet)—form a variety of microphase-separated shapes

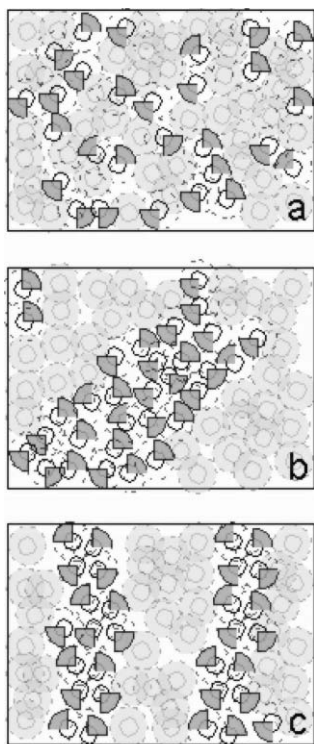


**Fig. 7** Solvation structures on a smectic layer interface. The small circles represent the POBC mesogen cores viewed end on; the diffuse grey circle represents the 2-D space pervaded by the inactive tail chain in its *up* sense; the dark quadrants are the more restricted space pervaded by the active  $\alpha$ -substituted tails in its *up* sense. **a.** Shows a random mixture of the two tail types; **b.** Nanophase-separated rafts comprised of aggregates of a single mesogen sense (tail type); **c.** A striped nanophase-separated solvation structure with vertical rows of close-packed active tails alternating with rows of inactive tails.

including “rafts” and “stripe” phases. Here we consider the potential for spatial patterning of the two distinct ends of the mesogens exhibiting  $\text{SmC}_A^*$  and  $\text{SmC}_A$  phases. Starting from the well-accepted premise that the polar sense of mesogen orientation (*up versus down*) is random in fluid smectics, the two distinct tails of the POBC mesogens are tantamount to mixing two different components within each aliphatic stratum—the analogue of an aliphatic leaflet comprised of more than one type of lipid (or lipids plus cholesterol). We posit that the relative locations of these two components (inequivalent terminal chains) could be manifested on the layer interface. The mesogen’s terminal chains may differ from one another because of different lengths ( $m \neq n$  in the POBC homologues). But the differences go beyond mere inequivalent chain-length and chain-parity: substitution on the  $\alpha$ -carbon with a single methyl (*e.g.*, the chiral  $\text{M}_n\text{PBOC}$  homologues), with two tails in swallow tail mesogens, or two methyls (*e.g.*, the new  $\text{DM}_n\text{PBOC}$  mesogens reported herein), imparts additional idiosyncratic conformational differences to the tails. That is, the tails are further differentiated from one another by their (average) excluded volumes: substitution restricts isomerization and the resulting average tail cross-sectional areas. Additionally there is the concomitant propensity for reinforcing a nonlinear mesogen shape that substitution on the  $\alpha$ -carbon of the tail imparts. Substitution close to the mesogenic core reinforces the persistence of the  $\sim 120^\circ$  “valence angle” at the tail-core junction. All of these considerations result in different attributes of the two tails and thereby further distinguish the *up* versus the *down* mesogen sense. Here, following the contemporary ideas in biophysics of mixed membrane, we suggest this distinction between the mesogenic tails could be especially important within the tail stratum of the smectic layer.

In summary, tail solvation patterns might imprint (complementary) topographical patterns on the smectic layer interfaces. We attempt to illustrate this in Fig. 7 showing some simple examples of the 2-D arrangement of the two distinct ends of a mesogen. Fig. 7a illustrates random mixing with no solvation structure. A nanophase-separated raft is shown in Fig. 7b. Fig. 7c is a striped arrangement in which the two different chain ends (with different excluded volumes and propensities for interdigitation) alternate in vertical rows. We hypothesize that these latter more structured arrangements result in a topographic pattern on the interface, and this pattern can communicate tilt preferences from layer-to-layer. This microscopic mechanism would apply to the entire class of known  $\text{SmC}_A$ -phase-forming mesogens from the original, chiral, methyl-substituted tails in the family of POBC mesogens to the related swallow-tail mesogens. It is advanced here without experimental corroboration in an effort to prompt further experiments, *e.g.*, evidence for such a patterned topology may be sought with atomic force microscopy or freeze-fracture electron microscopy.

### Acknowledgements

This work was supported by NSF grant DMR-9971143 and NASA University Research, Engineering and Technology Institute on Bio Inspired Materials (BIMat) under award no. NCC-1-02037; the Office of Naval Research MURI Grant N00014-98-1-0597rt supported equipment used in this research.

### References

- 1 J. Watanabe and M. Hayashi, *Macromolecules*, 1989, **22**, 4083.
- 2 A. D. L. Chandani, E. Gorecka, Y. Ouchi, H. Takezoe and A. Fukuda, *Jpn. J. Appl. Phys.*, 1989, **28**, L1265.
- 3 K. Miyachi and A. Fukuda, in *Handbook of Liquid Crystals*, ed. D. Demus, J. Goodby, G. W. Gray, H.-W. Spiess, and V. Vill, Wiley-VCH, Weinheim, 1998, **2B**, 665.
- 4 T. Matsumoto, A. Fukuda, M. Jhono, Y. Motoyama, T. Yui, S.-S. Seomun and M. Yamashita, *J. Mater. Chem.*, 1999, **9**, 2051.
- 5 Y. Takanishi, K. Hiraoka, V. K. Agrawal, H. Takezoe, A. Fukuda and M. Matsushita, *Jpn. J. Appl. Phys.*, 1991, **30**, L2023.
- 6 K. Hori and K. Endo, *Bull. Chem. Soc. Japan*, 1993, **66**, 46; K. Hori, S. Kawahara and K. Ito, *Ferroelectrics*, 1993, **147**, 91.
- 7 H. Toriumi, M. Yoshida, M. Mikami, M. Takeuchi and A. Mochizuki, *J. Phys. Chem.*, 1996, **100**, 15207; H. Toriumi, M. Yoshida, N. Kamiya and M. Takeuchi, *Mol. Cryst. Liq. Cryst.*, 2003, **402**, 267.
- 8 M. A. Osipov and A. Fukuda, *Phys. Rev. E*, 2000, **62**(3), 3724.
- 9 A. Fukuda, Y. Takanishi, T. Isozaki, K. Ishikawa and H. Takezoe, *J. Mater. Chem.*, 1994, **4**, 997.
- 10 I. Nishiyama and J. W. Goodby, *J. Mater. Chem.*, 1992, **2**, 1015.
- 11 M. Glaser and N. A. Clark, *Phys. Rev. E*, 2002, **66**, 21711.
- 12 Y. Takanishi, H. Takezoe, A. Fukuda, H. Komuara and J. Watanabe, *J. Mater. Chem.*, 1992, **2**, 71.
- 13 Y. Takanishi, H. Takezoe, A. Fukuda and J. Watanabe, *Phys. Rev. B*, 1992, **45**, 7684.
- 14 Y. Ouchi, Y. Yoshioka, H. Ishii, K. Seki, M. Kitamura, R. Noyori, Y. Takanishi and I. Nishiyama, *Mater. Chem.*, 1995, **5**(12), 2297.
- 15 J. P. F. Lagerwall, F. Giesselmann and M. D. Radcliffe, *Phys. Rev. E*, 2002, **66**, 31703.
- 16 A. Ikeda, Y. Takanishi, H. Takezoe and A. Fukuda, *Jpn. J. Appl. Phys.*, 1993, **32**, L97.
- 17 K. Uno, N. Nakamura, H. Toriumi, J. Thisayukta and E. T. Samulski, (in preparation).
- 18 Y. Takanishi, A. Ikeda, H. Takezoe and A. Fukuda, *Phys. Rev. E*, 1995, **51**, 400.
- 19 G. W. Gray and J. W. Goodby, *Mol. Cryst. Liq. Cryst.*, 1976, **37**, 157.
- 20 G. Pelzl, S. Diele and W. Weissflog, *Adv. Materials*, 1999, **11**, 707.
- 21 T. Dingemans, private communication (2003).
- 22 J. Xu, R. L. B. Singer, J. V. Selinger, B. R. Ratner and R. Shashidhar, *Phys. Rev. E*, 1999, **60**, 5584.
- 23 H. M. McConnell and M. Vrljic, *Annu. Rev. Biophys. Biomol. Struct.*, 2003, **32**, 469.